

THE SELECTION OF REVERSIBLE INTEGER-TO-INTEGERS WAVELET TRANSFORMS FOR DEM MULTI-SCALE REPRESENTATION AND PROGRESSIVE COMPRESSION

ZHENG Jing-jing^{a,b,*}, FANG Jin-yun^a, HAN Cheng-de^a

^aInstitute of Computing Technology, Chinese Academy of Sciences, Beijing 100190, China - zhengjingjing@ict.ac.cn

^bGraduate University of Chinese Academy of Sciences, Beijing 100190, China

Commission IV, WG IV/5

KEY WORDS: DEM; Multi-scale Representation; Compression; Geographical Services; Web Based

ABSTRACT:

In web based GIS visual simulation systems, the DEM multi-scale presentation and lossy-to-lossless progressive compression and transmission based on integer-to-integer wavelet transforms can eliminate the redundant data between resolutions. Therefore, it can relieve effectively the contradiction between the voluminous DEM data set and the limited network bandwidth. Among the many integer-to-integer wavelet transforms, which one is the most suitable to the DEM multi-scale representation and compression with high accuracy in every resolution has not been set forth. Thus, 15 different reversible integer-to-integer wavelet transforms are compared when compressing the DEM data with multi-scale progressive characteristic via the JPEG2000 algorithm, and these comparisons are mainly focused on their accuracy performance of maintaining the main original terrain characters in different resolutions. The terrain accuracy parameters are selected elaborately to better indicate the accuracy performance of different wavelet transforms. These transforms' lossless compression performance and computational complexity are also considered. Through a lot of experimental data and analyses, the 2/6 integer wavelet transform is found to be the most suitable transform for the DEM multi-scale representation and progressive compression. Factors affecting these performances are also discussed through theoretical arguments, which could be a guide to design new and more effective integer wavelet transforms for DEM progressive compression.

1. INTRODUCTION

Web-based GIS visual simulation systems have to handle voluminous elevation data sets, but the limited network bandwidth is a bottleneck. One commonly used method to solve this problem is that the data servers provide DEM multi-scale representations stored and compressed independently and transmit corresponding scale data according to the needs of clients. For example, Rishe et al. (2004) derived different resolution DEM data from the original resolution data and stored independently in server to provide the client different scale DEM data. However, in this method, there are a lot of redundant data between different resolutions because of the independence between different resolutions.

In recent years, wavelet transforms have been successfully used for images encoding. The multi-resolution nature of the transform, without redundancy between resolutions, is ideal for image data multi-resolution progressive compression and transmission. Therefore, the multi-resolution progressive compression method based on wavelet transform has been used in a few compression algorithms, for example, the EBCOT algorithm (Taubman, 2000) and the EZBC algorithm (Hsiang, 2001), and these algorithms are now mainly used to compress image and video data. For example, the new generation still image compression standard JPEG2000 (Bolic et al., 2000) is based on the EBCOT algorithm.

The DEM data can be considered as grey image data, so above multi-resolution progressive compression method is an ideal way to relieve effectively the contradiction between the voluminous DEM data sets and the limited network bandwidth. Because the DEM data needs high fidelities, lossy-to-lossless

progressive compression should be supported. However, the conventional wavelet filters often have floating point coefficients and couldn't realize the lossless reconstruction. The second generation wavelet transforms based on lifting scheme (Sweldens, 1996) map integers to integers and realize the lossless compression of DEM data with minimal memory usage and low computational complexity. What is more, the multi-scale progressive compression based on integer wavelets can easily allow the transmission of low resolution versions firstly, followed by transmissions of successive details.

Among the many different integer-to-integer wavelet transforms, which one is the most suitable to the DEM multi-scale representation and compression with high accuracy in every resolution has not been set forth in relative papers so far. Adams and Kossentini (2000) compared and analysed the image compression performance of 12 integer-to-integer wavelet transforms commonly used. However, this paper mainly aimed to the common still images. The DEM data have some particular characters different from regular optical images, such as the higher correlation between adjacent values and higher accuracy demand at different resolutions. Therefore, the most suitable specific integer wavelet transform that meets above needs should be chosen through further research in depth. However, as far as we know, current available researches have not solved this problem perfectly. Ottoson (2001) compressed the DEM data with only the DB6 conventional wavelet without comparing with other wavelets according to the characters of DEM data, and in addition the compression was lossy. Chen and Li (2007) only simply used the 5/3 integer transform which is commonly used in lossless image compression to compress DEM data, also without comparing with other integer wavelet transforms. Liu et al. (2005) considered these wavelets'

accuracy performance in different resolutions, but they simply compared 4 conventional wavelets using only one DEM experimental data and comparing only one resolution, and the accuracy parameters they used that indicated the accuracy performance of maintaining the main original terrain characters in different resolutions were also too simple.

Thus, in this paper 15 different reversible integer-to-integer wavelet transforms are compared on the basis of their accuracy performance of maintaining the main original terrain characters in different resolutions when compressing the DEM data with multi-scale progressive method. The terrain accuracy parameters are selected elaborately to better indicate the accuracy performance of different wavelet transforms. At the same time, these transforms' lossless compression performance and computational complexity are also considered. In addition, factors affecting these performances are discussed, supported by both experimental data and theoretical arguments.

2. INTEGER WAVELET TRANSFORMS AND COMPUTATIONAL COMPLEXITY

2.1 Integer wavelet transform

The reversible integer-to-integer wavelet transforms considered in this study were constructed using the technique described in Calderbank et al. (1998). In all, 15 transforms known to be effective for image coding were evaluated for the DEM data progressive compression. All of these transforms are strictly one-dimensional (1-D) in nature and are based on two-channel filter banks. The DEM data are handled by transforming the rows and columns in succession and the inverse transform must operate in the reverse order. The forward transform equations for each of the transforms are given as follows (Adams and Kossentini, 2000; Fang et al., 1998; Calderbank et al., 1998). The input signal, low pass sub-band signal, and high pass sub-band signal are denoted as $x[n]$, $s[n]$, and $d[n]$, respectively. For convenience, $s_0[n] = x[2n]$ and $d_0[n] = x[2n+1]$ are defined. The inverse transformation equations can be trivially deduced from the forward transformation equations, and thus are not given. Here, the notation m/n represents a transform with m coefficients in the low pass analysis filter and n coefficients in the high pass analysis filter. The notation (x, y) represents a transform with x and y vanishing moments in the analysis and synthesis high pass filters respectively.

15 integer-to-integer wavelet transforms compared:

S transform (1, 1) :

$$\begin{aligned} d[n] &= d_0[n] - s_0[n] \\ s[n] &= s_0[n] + \frac{1}{2}d_1[n] \end{aligned}$$

5/3 transform (2, 2) :

$$\begin{aligned} d[n] &= d_0[n] - \frac{1}{2}(s_0[n+1] + s_0[n]) \\ s[n] &= s_0[n] + \frac{1}{4}(d[n] + d[n-1]) + \frac{1}{2} \end{aligned}$$

2/6 transform (3, 1) :

$$\begin{aligned} d_1[n] &= d_0[n] - s_0[n] \\ s[n] &= s_0[n] + \frac{1}{2}d_1[n] \\ d[n] &= d_1[n] + \frac{1}{4}(-s[n+1] + s[n-1]) + \frac{1}{2} \end{aligned}$$

SPB transform :

$$\begin{aligned} d_1[n] &= d_0[n] - s_0[n] \\ s[n] &= s_0[n] + \frac{1}{2}d_1[n] \\ d[n] &= d_1[n] + \frac{1}{8}(-3s[n+1] + s[n] + 2s[n-1] + 2d_1[n+1]) + \frac{1}{2} \end{aligned}$$

9/7-M transform (4, 2) :

$$\begin{aligned} d[n] &= d_0[n] + \frac{1}{16}((s_0[n+2] + s_0[n-1]) - 9(s_0[n+1] + s_0[n])) + \frac{1}{2} \\ s[n] &= s_0[n] + \frac{1}{4}(d[n] + d[n-1]) + \frac{1}{2} \end{aligned}$$

(2, 4) transforms :

$$\begin{aligned} d[n] &= d_0[n] - \frac{1}{2}(s[n] + s[n+1]) + \frac{1}{2} \\ s[n] &= s_0[n] + \frac{19}{64}(d[n-1] + d[n]) - \frac{3}{64}(d[n-2] + d[n+1]) + \frac{1}{2} \end{aligned}$$

(6, 2) transform :

$$\begin{aligned} d[n] &= d_0[n] - \left[\frac{75}{128}(x[n] + x[n+1]) - \frac{25}{256}(x[n-1] + x[n+2]) + \frac{3}{256}(x[n-2] + x[n+3]) + \frac{1}{2} \right] \\ s[n] &= s_0[n] + \frac{1}{4}(d[n-1] + d[n]) + \frac{1}{2} \end{aligned}$$

13/7-T transform (4, 4) :

$$\begin{aligned} d[n] &= d_0[n] + \frac{1}{16}((s_0[n+2] + s_0[n-1]) - 9(s_0[n+1] + s_0[n])) + \frac{1}{2} \\ s[n] &= s_0[n] + \frac{1}{32}(-d[n+1] - d[n-2] + 9(d[n] + d[n-1])) + \frac{1}{2} \end{aligned}$$

5/11-C transform (2+2, 2):

$$\begin{aligned} d_1[n] &= d_0[n] - \frac{1}{2}(s_0[n+1] + s_0[n]) \\ s[n] &= s_0[n] + \frac{1}{4}(d_1[n] + d_1[n-1]) + \frac{1}{2} \\ d[n] &= d_1[n] + \frac{1}{16}(s_1[n+2] - s_1[n+1] - s_1[n] + s_1[n-1]) + \frac{1}{2} \end{aligned}$$

2/10 transform (5, 1) :

$$\begin{aligned} d_1[n] &= d_0[n] - s_0[n] \\ s[n] &= s_0[n] + \frac{1}{2}d_1[n] \\ d[n] &= d_1[n] + \frac{1}{64}(22(s[n-1] - s[n+1]) + 3(s[n+2] - s[n-2])) + \frac{1}{2} \end{aligned}$$

5/11-A transform (2, 2) :

$$\begin{aligned} d_1[n] &= d_0[n] - \frac{1}{2}(s_0[n+1] + s_0[n]) \\ s[n] &= s_0[n] + \frac{1}{4}(d_1[n] + d_1[n-1]) + \frac{1}{2} \\ d[n] &= d_1[n] + \frac{1}{32}(s_1[n+2] - s_1[n+1] - s_1[n] + s_1[n-1]) + \frac{1}{2} \end{aligned}$$

6/14 transform (3, 3) :

$$\begin{aligned} d_1[n] &= d_0[n] - s_0[n] \\ s[n] &= s_0[n] + \frac{1}{16}(-d_1[n+1] + d_1[n-1] + 8d_1[n]) + \frac{1}{2} \\ d[n] &= d_1[n] + \frac{1}{16}(s_1[n+2] - s_1[n-2] + 6(-s_1[n+1] + s_1[n-1])) + \frac{1}{2} \end{aligned}$$

SPC transform :

$$\begin{aligned} d_1[n] &= d_0[n] - s_0[n] \\ s[n] &= s_0[n] + \frac{1}{2}d_1[n] \\ d[n] &= d_1[n] + \frac{1}{16}(-8s[n+1] + 4s[n] + 5s[n-1] - s[n-2] + 6d_1[n+1]) + \frac{1}{2} \end{aligned}$$

13/7-C transform (4, 2) :

$$\begin{aligned} d[n] &= d_0[n] + \frac{1}{16}((s_0[n+2] + s_0[n-1]) - 9(s_0[n+1] + s_0[n])) + \frac{1}{2} \\ s[n] &= s_0[n] + \frac{1}{16}(5(d[n] + d[n-1]) - (d[n+1] + d[n-2])) + \frac{1}{2} \end{aligned}$$

9/7-F transform (4, 4) :

$$\begin{aligned} d_1[n] &= d_0[n] + \frac{203}{128}(-s_0[n+1] - s_0[n]) + \frac{1}{2} \\ s_1[n] &= s_0[n] + \frac{217}{4096}(-d_1[n] - d_1[n-1]) + \frac{1}{2} \\ d[n] &= d_1[n] + \frac{113}{128}(s_1[n+1] + s_1[n]) + \frac{1}{2} \\ s[n] &= s_1[n] + \frac{1817}{4906}(d[n] + d[n-1]) + \frac{1}{2} \end{aligned}$$

2.2 Computational complexity

For the purpose of decreasing and analysing the computational complexity, all above transforms' denominators can be written as 2^N , which can be implemented as the arithmetic right shift of denominators by N bits. Using Booth's algorithm (Booth, 1951), all the multiplications in the numerators are converted to shift and add operations. Thus all the operations are only adds and shifts, which is simple to evaluate these transforms' computational complexity. By assuming the one-level wavelet decomposition (in one dimension), the number of addition and shift operations required per two input samples for each transform is given in Table 1.

Transform	Adds	Shifts	Total
S	2	1	3
5/3	5	2	7
2/6	5	2	7
SPB	8	3	11
9/7-M	9	3	12
(2, 4)	10	5	15
(6, 2)	16	9	25
13/7-T	12	4	16
5/11-C	10	3	13
2/10	10	6	16
5/11-A	10	3	13
6/14	11	5	16
SPC	10	5	15
13/7-C	12	4	16
9/7-F	26	18	44

Table 1. 15 integer wavelets' computational complexity

3. INTEGER WAVELET TRANSFORM EXPERIMENTS, ANALYSES AND SELECTION

In this paper, above 15 reversible integer wavelet transforms are compared on the basis of their accuracy performance of maintaining the main original terrain characters in different resolutions when compressing the DEM data with multi-scale progressive method. The terrain accuracy parameters are selected elaborately to better indicate the accuracy performance of different wavelet transforms. At the same time, the lossless compression performance and computational complexity of these transforms are also considered.

For evaluation purpose, the JPEG2000 open source software OpenJPEG lib (Janssens, 2007) was employed to compress DEM data losslessly. Because much of the function required for our analyses was not present, the original transform-related code in the software was replaced with new code to facilitate our testing. After the integer lifting transform, the coefficients with multi-resolution characteristic are bitplane and entropy coded with the resolution progressive compression character.

The experimental data were from SRTM 90m DEM data (Jarvis et al. 2006). The projection is transverse Mercator and the grid interval is 90m×90m. Three sample DEM data DEM1, DEM2, and DEM3, with different terrain types and sizes, were employed. The top upper latitude and longitude of DEM1 are 35° N. and 107.5° E., and the map sheet size is 512×512. The (35° N., 110° E.) is the DEM2's top upper coordinate, and the

(35° N., 112.5° E) is the DEM3's top upper coordinate. The DEM2 and DEM3 are all 1200 × 1800 in size.

3.1 Accuracy performance experiments and analyses

In order to better evaluate these transforms' accuracy performance of maintaining the main original terrain characteristics in different resolutions, the accuracy performance indicators have to be selected elaborately. Currently there is no uniform measure criterion about the DEM accuracy. Liu et al. (2005) simply used the elevations' maximum value, minimum value, mean value, and standard derivation, and these parameters were too simple. Tang et al. (2001) had put forward the concept of DEM terrain representation error (Et) and had investigated the generation, major factors, measurement and simulation of Et. Through many experiments and analyses, they revealed that the Et root mean square error (RMS Et) value has a positive quantitative relationship with the DEM resolution and the terrain roughness at global levels. The terrain roughness can be indicated by mean profile curvature. It was found that the RMS Et can be expressed as follows:

$$\text{RMS Et} = (0.0063R - 0.022)V + 0.0066R + 0.2415$$

Where R = terrain resolution ($\geq 10m$)
 V = mean profile curvature

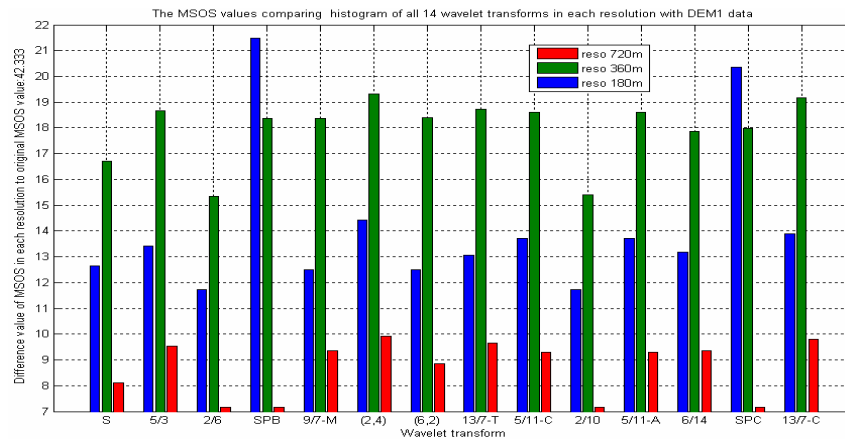
It has been proved that the digital matrix of the terrain profile curvature can be obtained by computing the slope of the terrain's slope. Thus, the mean profile curvature can be obtained by computing the mean slope of slope (MSOS). Therefore, the MSOS value was chosen to be the most important parameter to measure the DEM accuracy performance. Other parameters measuring the accuracy performance are the elevation's minimum value, maximum value, mean value, and standard derivation.

Among these 15 integer wavelet transforms, although the 9/7-F transform was proved to be effective in lossy compression, but performed poorly in lossless compression (Michael et al., 2000). In addition, as shown in table 1, it needs 44 operations in each transform step and its complexity is the highest. What is more, through experiments on the DEM2 progressive compression using this transform, it was found that the dynamic range after reconstruction in each resolution was different far from the original data range. Thus, considering all above factors, the 9/7-F transform wasn't included in the succeeding experiments.

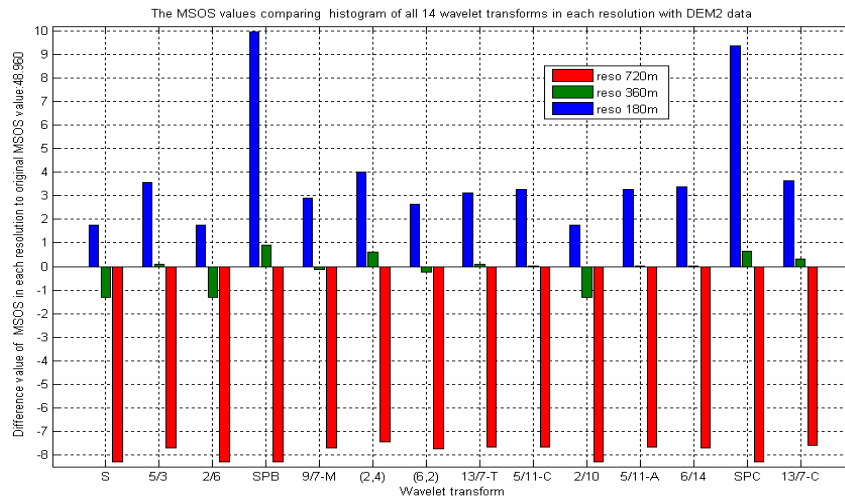
First of all, the MSOS values, as the most important DEM accuracy measuring parameter, were computed and compared in the same resolution of all the 14 transforms to a certain tested DEM data. Each DEM data was decomposed to 4 resolutions with 3 levels wavelet decomposition of each transforms. For each DEM data, all the 3 resolutions' MSOS values were computed and compared except the fourth full resolution, and these values are showed in one figure. Figure 1 (a), (b), and (c) show the experimental results of DEM1, DEM2 and DEM3 respectively. To facilitate compare, the original resolution's MSOS value is subtracted from each MSOS value in each resolution of each wavelet, and the original MSOS value is given in each figure. Because the RMS Et has a positive quantitative relationship with the MSOS value, the least the MSOS value, the least the RMS Et. Through compare, it could

be concluded that the 2/6 integer wavelet generally performs best considering all resolutions of all the tested data, followed closely by the 2/10 and S transforms. Then the next 3

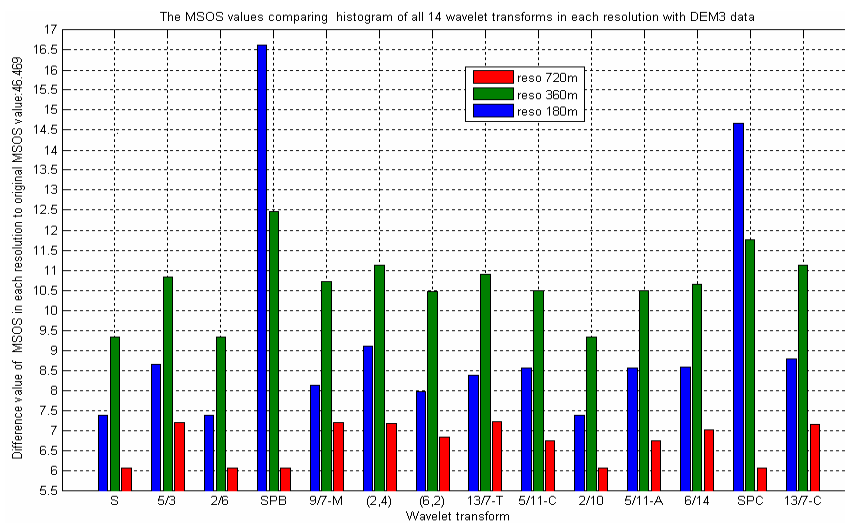
transforms in turn are the SPC, SPB, and (6, 2) transform in decreasing order of the RMS Et accuracy performance.



(a) DEM1



(b) DEM2



(c) DEM3

Figure 1. The MSOS values comparing histogram of DEM1 (a), DEM2 (b) and DEM3 (c)

Data	Reso	Wavelet	Min	Max	Mean	Std dev	
DEM1	90m	Original	600	1406	963.59	144.33	
		S	596	1407	<i>963.614</i>	<i>144.337</i>	
		2/6	<i>600</i>	1401	963.332	144.207	
		SPB	585	1402	963.541	144.388	
		(6,2)	599	<i>1406</i>	963.993	144.549	
		2/10	<i>600</i>	1401	963.332	144.207	
	180m	SPC	S	592	<i>1404</i>	<i>963.646</i>	<i>144.385</i>
			2/6	<i>600</i>	1390	963.028	143.863
			SPB	594	1389	963.098	143.974
			(6,2)	595	1399	964.774	144.969
			2/10	<i>600</i>	1390	963.028	143.863
			SPC	588	1392	963.107	144.051
	360m	S	2/6	<i>600</i>	1367	962.659	142.977
			SPB	<i>600</i>	1367	962.659	142.977
			(6,2)	589	1363	966.190	145.644
			2/10	<i>600</i>	1367	962.659	142.977
			SPC	<i>600</i>	1367	962.659	142.977
			720m	S	2/6	<i>600</i>	1367
	SPB	<i>600</i>			1367	962.659	142.977
	(6,2)	182			2310	804.644	325.227
	2/6	<i>182</i>			2301	804.299	325.073
	SPB	168			2328	<i>804.423</i>	325.312
	(6,2)	<i>182</i>			<i>2304</i>	804.904	<i>325.290</i>
	180m	2/10	SPC	144	2353	804.421	325.456
S			<i>182</i>	2294	803.915	324.634	
2/6			<i>182</i>	2294	803.915	324.634	
SPB			<i>182</i>	<i>2307</i>	<i>803.954</i>	324.787	
(6,2)			184	2300	805.346	<i>325.356</i>	
2/10			<i>182</i>	2294	803.915	324.634	
360m	SPC	S	<i>183</i>	<i>2265</i>	<i>803.487</i>	323.501	
		2/6	<i>183</i>	<i>2265</i>	<i>803.487</i>	323.501	
		SPB	<i>183</i>	<i>2265</i>	<i>803.487</i>	323.501	
		(6,2)	180	2264	806.078	<i>325.232</i>	
		2/10	<i>183</i>	<i>2265</i>	<i>803.487</i>	323.501	
		SPC	<i>183</i>	<i>2265</i>	<i>803.487</i>	323.501	
DEM2	90m	Original	70	1768	622.237	450.837	
		S	<i>70</i>	<i>1756</i>	621.967	450.692	
		2/6	<i>70</i>	<i>1756</i>	621.967	450.692	
		SPB	<i>70</i>	1742	<i>622.108</i>	<i>450.854</i>	
		(6,2)	<i>70</i>	1754	622.846	450.904	
		2/10	<i>70</i>	<i>1756</i>	621.967	450.692	
	180m	SPC	S	<i>70</i>	1786	622.085	450.970
			2/6	<i>70</i>	1736	621.651	450.367
			SPB	<i>70</i>	1736	621.651	450.367
			(6,2)	<i>70</i>	1727	<i>621.702</i>	450.461
			2/10	<i>70</i>	1736	621.651	450.367
			SPC	<i>70</i>	1718	621.689	450.530
	360m	S	2/6	<i>70</i>	<i>1682</i>	<i>621.273</i>	449.616
			SPB	<i>70</i>	<i>1682</i>	<i>621.273</i>	449.616
			(6,2)	71	<i>1696</i>	626.225	<i>451.013</i>
			2/10	<i>70</i>	<i>1682</i>	<i>621.273</i>	449.616
			SPC	<i>70</i>	<i>1682</i>	<i>621.273</i>	449.616
			720m	S	2/6	<i>70</i>	<i>1682</i>
	SPB	<i>70</i>			<i>1682</i>	<i>621.273</i>	449.616
	(6,2)	71			<i>1696</i>	626.225	<i>451.013</i>
	2/10	<i>70</i>			<i>1682</i>	<i>621.273</i>	449.616
	SPC	<i>70</i>			<i>1682</i>	<i>621.273</i>	449.616
	DEM3	90m			Original	70	1768
			S	<i>70</i>	<i>1756</i>	621.967	450.692
2/6			<i>70</i>	<i>1756</i>	621.967	450.692	
SPB			<i>70</i>	1742	<i>622.108</i>	<i>450.854</i>	
(6,2)			<i>70</i>	1754	622.846	450.904	
2/10			<i>70</i>	<i>1756</i>	621.967	450.692	
180m	SPC	S	<i>70</i>	1786	622.085	450.970	
		2/6	<i>70</i>	1736	621.651	450.367	
		SPB	<i>70</i>	1736	621.651	450.367	
		(6,2)	<i>70</i>	1727	<i>621.702</i>	450.461	
		2/10	<i>70</i>	1736	621.651	450.367	
		SPC	<i>70</i>	1718	621.689	450.530	
360m	S	2/6	<i>70</i>	<i>1682</i>	<i>621.273</i>	449.616	
		SPB	<i>70</i>	<i>1682</i>	<i>621.273</i>	449.616	
		(6,2)	71	<i>1696</i>	626.225	<i>451.013</i>	
		2/10	<i>70</i>	<i>1682</i>	<i>621.273</i>	449.616	
		SPC	<i>70</i>	<i>1682</i>	<i>621.273</i>	449.616	
		720m	S	2/6	<i>70</i>	<i>1682</i>	<i>621.273</i>
SPB	<i>70</i>			<i>1682</i>	<i>621.273</i>	449.616	
(6,2)	71			<i>1696</i>	626.225	<i>451.013</i>	
2/10	<i>70</i>			<i>1682</i>	<i>621.273</i>	449.616	
SPC	<i>70</i>			<i>1682</i>	<i>621.273</i>	449.616	
DEM3	90m			Original	70	1768	622.237
		S	<i>70</i>	<i>1756</i>	621.967	450.692	
		2/6	<i>70</i>	<i>1756</i>	621.967	450.692	
		SPB	<i>70</i>	1742	<i>622.108</i>	<i>450.854</i>	
		(6,2)	<i>70</i>	1754	622.846	450.904	
		2/10	<i>70</i>	<i>1756</i>	621.967	450.692	
180m	SPC	S	<i>70</i>	1786	622.085	450.970	
		2/6	<i>70</i>	1736	621.651	450.367	
		SPB	<i>70</i>	1736	621.651	450.367	
		(6,2)	<i>70</i>	1727	<i>621.702</i>	450.461	
		2/10	<i>70</i>	1736	621.651	450.367	
		SPC	<i>70</i>	1718	621.689	450.530	
360m	S	2/6	<i>70</i>	<i>1682</i>	<i>621.273</i>	449.616	
		SPB	<i>70</i>	<i>1682</i>	<i>621.273</i>	449.616	
		(6,2)	71	<i>1696</i>	626.225	<i>451.013</i>	
		2/10	<i>70</i>	<i>1682</i>	<i>621.273</i>	449.616	
		SPC	<i>70</i>	<i>1682</i>	<i>621.273</i>	449.616	
		720m	S	2/6	<i>70</i>	<i>1682</i>	<i>621.273</i>
SPB	<i>70</i>			<i>1682</i>	<i>621.273</i>	449.616	
(6,2)	71			<i>1696</i>	626.225	<i>451.013</i>	
2/10	<i>70</i>			<i>1682</i>	<i>621.273</i>	449.616	
SPC	<i>70</i>			<i>1682</i>	<i>621.273</i>	449.616	
DEM3	90m			Original	70	1768	622.237
		S	<i>70</i>	<i>1756</i>	621.967	450.692	
		2/6	<i>70</i>	<i>1756</i>	621.967	450.692	
		SPB	<i>70</i>	1742	<i>622.108</i>	<i>450.854</i>	
		(6,2)	<i>70</i>	1754	622.846	450.904	
		2/10	<i>70</i>	<i>1756</i>	621.967	450.692	
180m	SPC	S	<i>70</i>	1786	622.085	450.970	
		2/6	<i>70</i>	1736	621.651	450.367	
		SPB	<i>70</i>	1736	621.651	450.367	
		(6,2)	<i>70</i>	1727	<i>621.702</i>	450.461	
		2/10	<i>70</i>	1736	621.651	450.367	
		SPC	<i>70</i>	1718	621.689	450.530	
360m	S	2/6	<i>70</i>	<i>1682</i>	<i>621.273</i>	449.616	
		SPB	<i>70</i>	<i>1682</i>	<i>621.273</i>	449.616	
		(6,2)	71	<i>1696</i>	626.225	<i>451.013</i>	
		2/10	<i>70</i>	<i>1682</i>	<i>621.273</i>	449.616	
		SPC	<i>70</i>	<i>1682</i>	<i>621.273</i>	449.616	
		720m	S	2/6	<i>70</i>	<i>1682</i>	<i>621.273</i>
SPB	<i>70</i>			<i>1682</i>	<i>621.273</i>	449.616	
(6,2)	71			<i>1696</i>	626.225	<i>451.013</i>	
2/10	<i>70</i>			<i>1682</i>	<i>621.273</i>	449.616	
SPC	<i>70</i>			<i>1682</i>	<i>621.273</i>	449.616	
DEM3	90m			Original	70	1768	622.237
		S	<i>70</i>	<i>1756</i>	621.967	450.692	
		2/6	<i>70</i>	<i>1756</i>	621.967	450.692	
		SPB	<i>70</i>	1742	<i>622.108</i>	<i>450.854</i>	
		(6,2)	<i>70</i>	1754	622.846	450.904	
		2/10	<i>70</i>	<i>1756</i>	621.967	450.692	
180m	SPC	S	<i>70</i>	1786	622.085	450.970	
		2/6	<i>70</i>	1736	621.651	450.367	
		SPB	<i>70</i>	1736	621.651	450.367	
		(6,2)	<i>70</i>	1727	<i>621.702</i>	450.461	
		2/10	<i>70</i>	1736	621.651	450.367	
		SPC	<i>70</i>	1718	621.689	450.530	
360m	S	2/6	<i>70</i>	<i>1682</i>	<i>621.273</i>	449.616	
		SPB	<i>70</i>	<i>1682</i>	<i>621.273</i>	449.616	
		(6,2)	71	<i>1696</i>	626.225	<i>451.013</i>	
		2/10	<i>70</i>	<i>1682</i>	<i>621.273</i>	449.616	
		SPC	<i>70</i>	<i>1682</i>	<i>621.273</i>	449.616	
		720m	S	2/6	<i>70</i>	<i>1682</i>	<i>621.273</i>
SPB	<i>70</i>			<i>1682</i>	<i>621.273</i>	449.616	
(6,2)	71			<i>1696</i>	626.225	<i>451.013</i>	
2/10	<i>70</i>			<i>1682</i>	<i>621.273</i>	449.616	
SPC	<i>70</i>			<i>1682</i>	<i>621.273</i>	449.616	

Table 2. Compare of elevation parameters

In addition, the elevation parameters (the elevation's minimum value, maximum value, mean value, and standard derivation) of the 2/6, 2/10, S, SPC, SPB, and (6, 2) transforms were further

compared using the same method. Table 2 shows the compare of these elevation parameters in each resolution of each DEM data. To facilitate compare, the best value of each parameter in each resolution of each DEM data is underlined, boldfaced and italic. It is found that there is not a unique wavelet filter that performs uniformly better than all the others for all the three resolutions and all the DEM data. For example, the (6, 2) transform performs the best among the 6 transforms for the 180m resolution of DEM2, but it performs poorly for the 360m resolution of DEM1. Some transforms have the same elevation parameters values for the same resolution of the same DEM data, and they are underlined, boldfaced and italic in table 2. Generally, the 2/6, 2/10, and S transforms have the close and even same elevation accuracy parameters and perform particularly well for all tested DEM data.

3.2 Compression performance and computational complexity performance experiments and analyses

The lossless compression performance and the computational complexity were also considered. The three DEM data were all compressed losslessly using the S, 2/6, 2/10, SPB, SPC and (6, 2) transforms. The average compressed file sizes (KB) and average compressing ratios for these 6 transforms are shown in table 3. To facilitate comparing the computational complexity, table 3 also shows the numbers of addition and shift operations having computed in table 1. From table 3, It can be concluded that, in the lossless compression ratio side, on average, the 2/6 transform increases 18.29% comparing with the S transform, decreases 4.54% with the 2/10 transform, decreases 1.69% with the SPB transform, decreases 5.96% with the SPC transform, and decrease 7.79% with the (6,2) transform.

DEM data and statistics	Original data size	S	2/6	2/10	SPB	SPC	(6, 2)

4. THEORETICAL ARGUMENTS

Factors affecting these experimental results and performances of these transforms are also examined from theoretical sides.

To the accuracy performance of maintaining the main terrain characteristics in different resolutions of different transforms, the most important affecting factor is the dynamic range of the forward transform coefficients in the low pass sub-band. The worst-case dynamic range growth of a particular transform is an approximate function of the 1-norm of its analysis filters. Since the different resolutions of the DEM data are owing to the successive wavelet decomposition of the low-pass sub-band signals, the 1-norm of the wavelet' low pass analysis filters is the most important factor affecting the accuracy performance of different resolutions and different wavelet transforms. Typically, the coefficients obtained by the decomposition of analysis filters have a greater dynamic range than original samples. Among the 15 transforms, only the 1-norms of the S, 2/6, 2/10, SPB, and SPC transforms' low pass analysis filters equal 1 and their transform coefficients have no dynamic range growth. This characteristic of these 5 transforms provides a greater possibility in obtaining excellent accuracy performance in each resolution of each DEM data. This point has been proved by the experimental results. For example, the S, 2/6, and 2/10 transforms perform well in the accuracy performance for all tested DEM data.

Besides the above factor, whether the transform has IIR filters is a negative factor to affect the accuracy performance. This point has been proved by the SPB and SPC transforms. Although they also have no dynamic range increase, they all have IIR filters. Thus they perform well to some data, but perform poorly to others.

To the lossless compression performance and computational complexity, the affecting factors have been covered by many researches (e.g. Adams and Kossentini, 2000), such as the number of vanishing moments, the shape and the lifting steps of wavelets. These factors also have been proved by our experiments. For example, the 2/6 transform has better compression performance than the S transform, because the 2/6 wavelet has 3 vanish moments while the S transform has only 1 vanish moment in the high pass analysis filters.

5. CONCLUSION

Thus, through experimental data, analyses and theoretical arguments, the 2/6 integer wavelet was found to be the most suitable transform for the DEM multi-scale representation and progressive compression among the 15 reversible integer-to-integer wavelet transforms compared. In addition, several factors affecting the accuracy performance and compression performance were also found, which could be a guide to design new and more effective integer wavelet transforms for the DEM multi-scale representation and progressive compression. In the future research, more DEM data with different terrain types and different sizes could be employed to strengthen the conclusion.

ACKNOWLEDGEMENTS

This research is supported by National Basic Research Program of China (2004CB318202) .

REFERENCES

- Adams, M. D., and Kossentini, F., 2000. Reversible Integer-to-Integer Wavelet Transforms for Image Compression: Performance Evaluation and Analysis. *IEEE Transactions on Image Processing*, 9(6), pp. 1010-1024.
- Boliek, M., Christopoulos, C., and Majani, E., (editors), 2000. JPEG2000 Part 1 Final Draft International Standard. *ISO/IEC FDIS 15444-1, ISO/IEC JTC1/SC29 WG1 N1855*.
- Booth, A. D., 1951. A signed binary multiplication technique. *Quar. J. Mech. Appl. Math.*, vol. 4, pp. 236-240.
- Calderbank, A. R., Daubechies, I., Sweldens W., and Yeo, B. 1998. Wavelet transforms that map integers to integers. *Applied and Computational Harmonic Analysis*. Vol. 5, pp. 332-369.
- Chen, R., and Li, X., 2007. DEM Compression Based on Integer Wavelet Transform. *Geo-spatial Information Science*, 10(2), pp. 133-136.
- Fang, S., Bilgin, A., Sementilli P. J., and Marcellin M. W., 1998. Lossy and lossless image compression using reversible integer wavelet transforms. *Proc. IEEE Int. Conf. Image Processing*, vol. 3, pp. 876-880.
- Hsiang, S. T., 2001. Embedded image coding using zeroblocks of subband/wavelet coefficients and context modelling. *Data Compression. Conf., DCC 2001, Proceedings*, pp. 662-665.
- Janssens, D., et al., 2007. OpenJPEG LIB. version 1.2, available from: <http://www.openjpeg.org>
- Jarvis A., Reuter, H.I., Nelson, A. and Guevara, E., 2006. Hole-filled seamless SRTM data V3. International Centre for Tropical Agriculture (CIAT). <http://srtm.csi.cgiar.org>.
- Liu, J., Zhu, Z., and Wang, J., 2005. The Impact of Multi-Scale Representation of DEM Derived From Different Wavelet Basis. *IEEE international proceedings on Geoscience and Remote Sensing Symposium, IGARSS 2005*, pp. 1694-1696.
- Ottoson, P., 2001. Compressing Digital Elevation Models with Wavelet Decomposition. *ScanGIS*, pp. 15-31.
- Rishe, N., Sun, Y., Chekmasov, M., et al. 2004. System Architecture for 3D TerraFly Online GIS. *Proceedings of the IEEE Sixth International Symposium on Multimedia Software Engineering, ISMSE'04*, pp. 273-276.
- Sweldens, W., 1996. The lifting Scheme: A Custom-design Construction of Biorthogonal Wavelets. *Applied and Computational Harmonic Analysis*, 3(2), pp. 186-200
- Tang, G. and Gong, J., et al., 2001. A Simulation on the Accuracy of DEM Terrain Representation. *Acta Geodaetica et Cartographica Sinica*, 30(1), pp. 361-365
- Taubman, D., 2000. High Performance Scalable Image Compression with EBCOT. *IEEE Transaction on Image Processing*, 9(7), pp. 1158-1170.